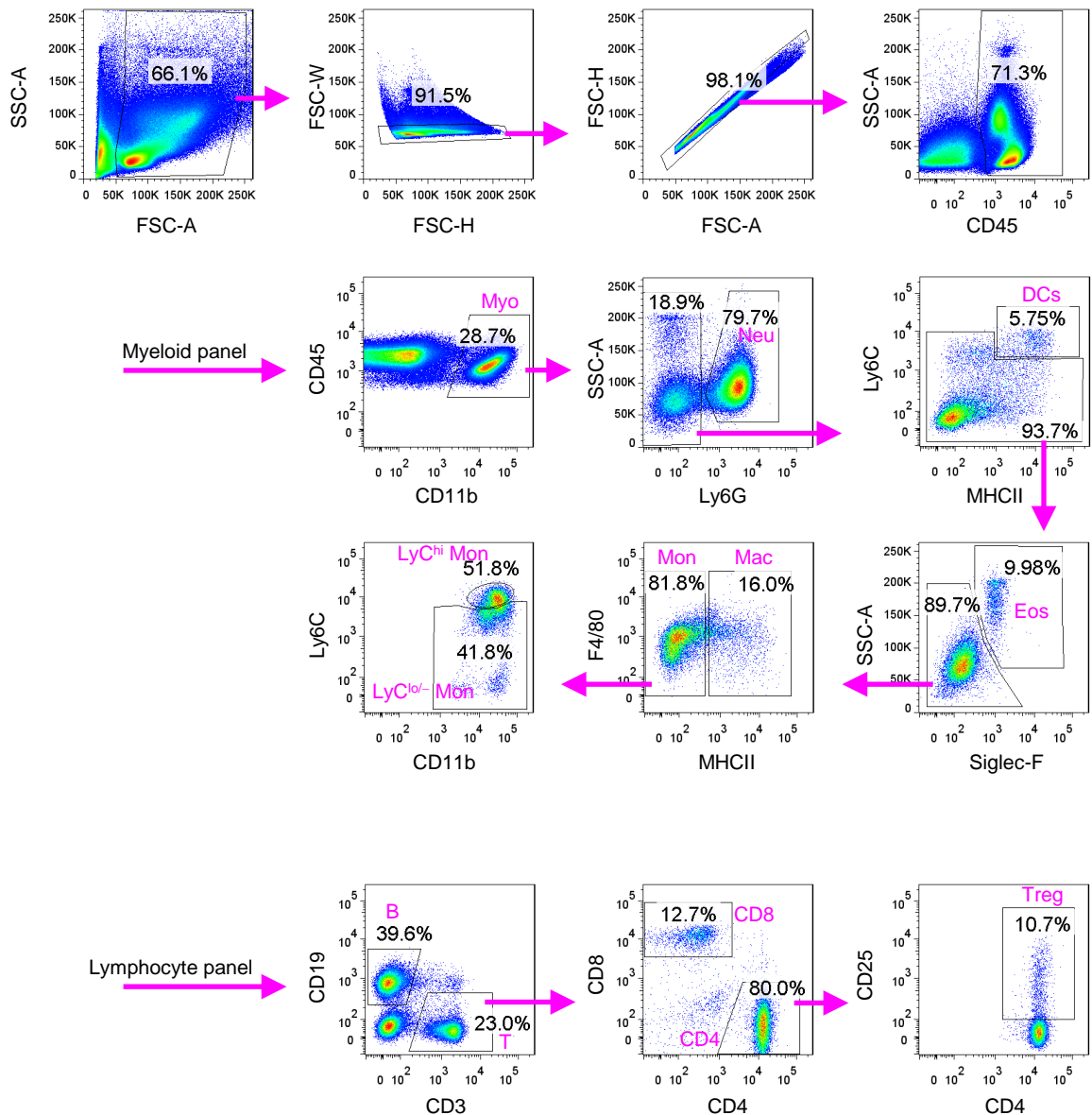
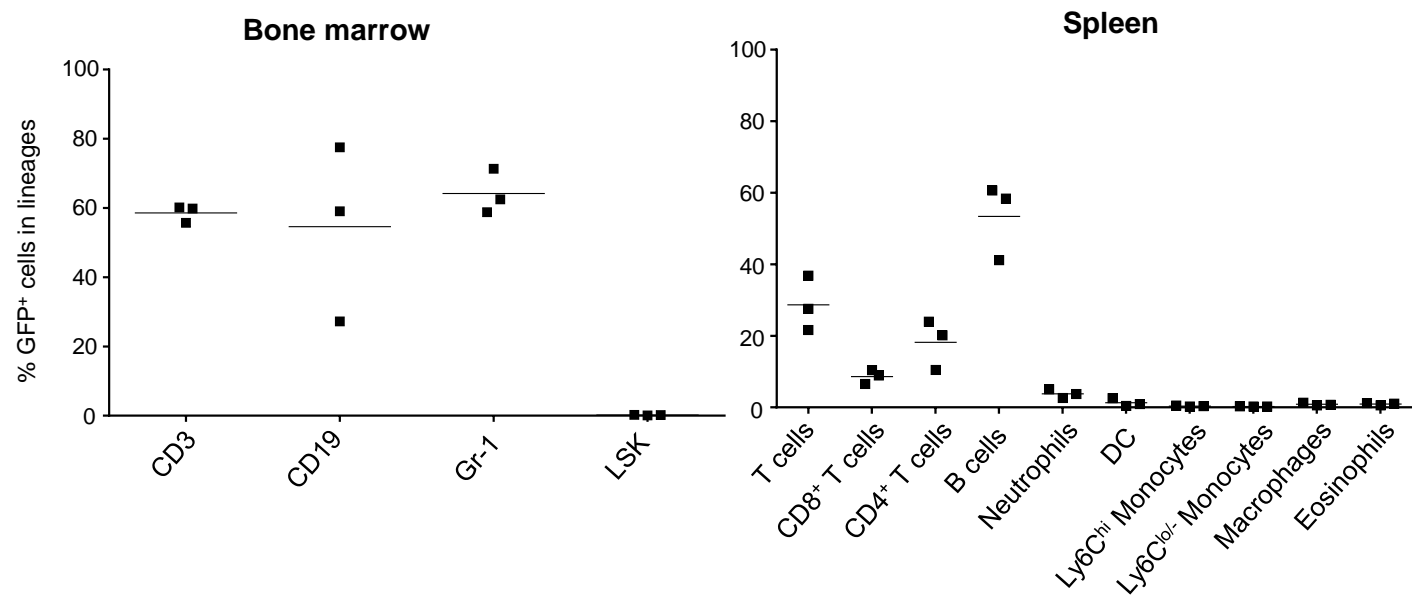


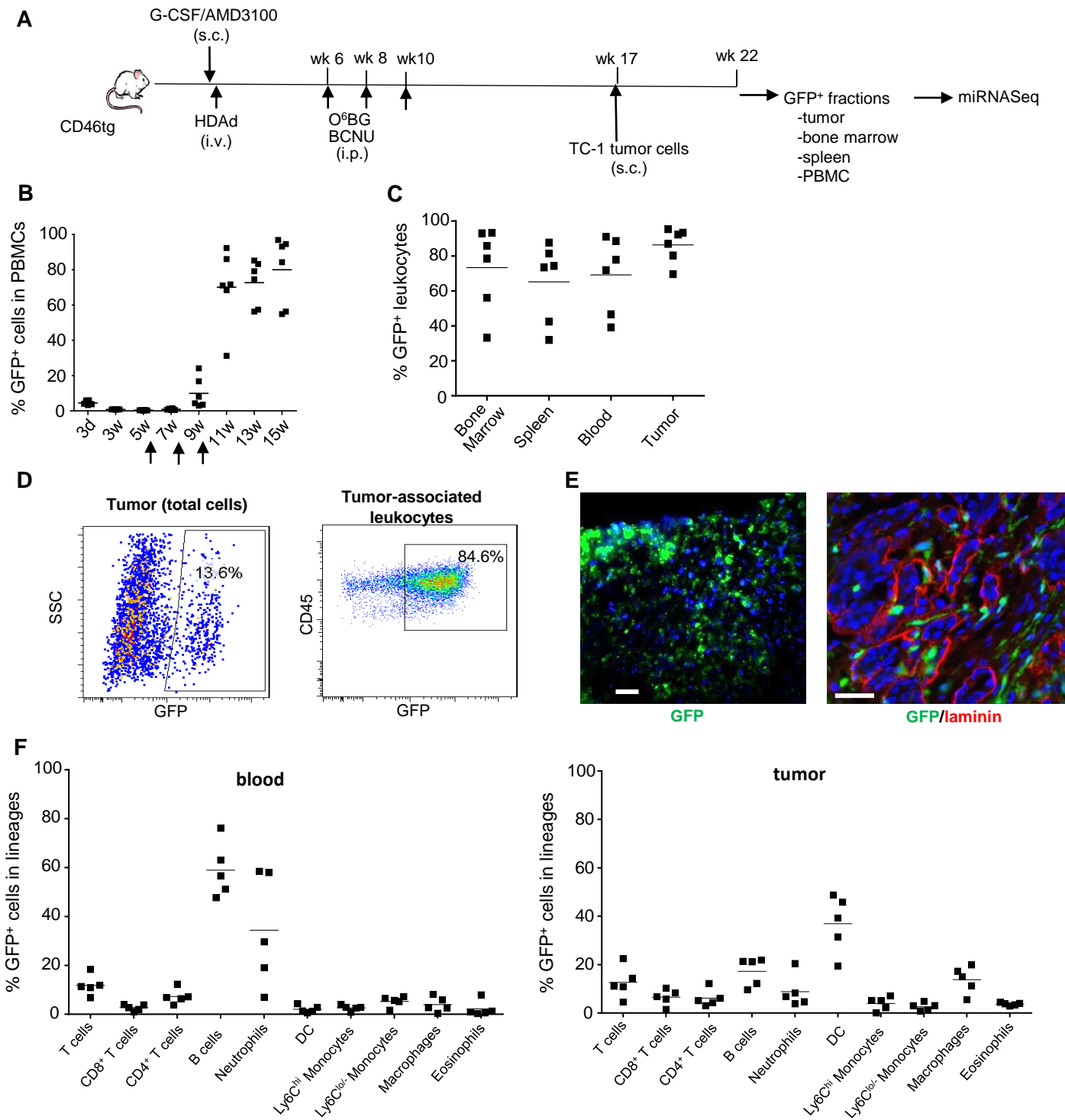
Supplementary Fig. S1. Rat Neu is expressed in MMC cells. Cells were stained with the Neu-specific monoclonal antibody 7.16.4 followed by anti-mouse Ig-FITC. Shown is a representative confocal microscopy image of cultured MMC cells. Neu-specific signals appear in green. The scale bar is 20μm.



Supplementary Fig. S2. Gating strategy used for immunophenotyping. Neu-neutrophils; DCs-dendritic cells; Mon-monocytes; Mac-macrophages; Eos-eosinophils; Treg-regulatory T-cells

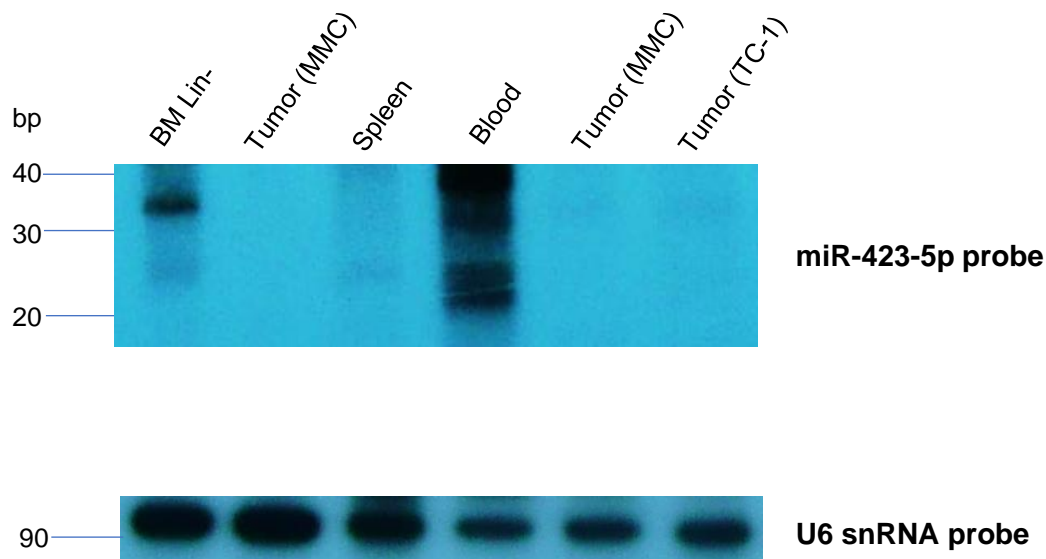


Supplementary Fig. S3. Immunophenotyping of GFP⁺ cells in the bone marrow and spleen (MMC model). For details, see Fig. 1D.

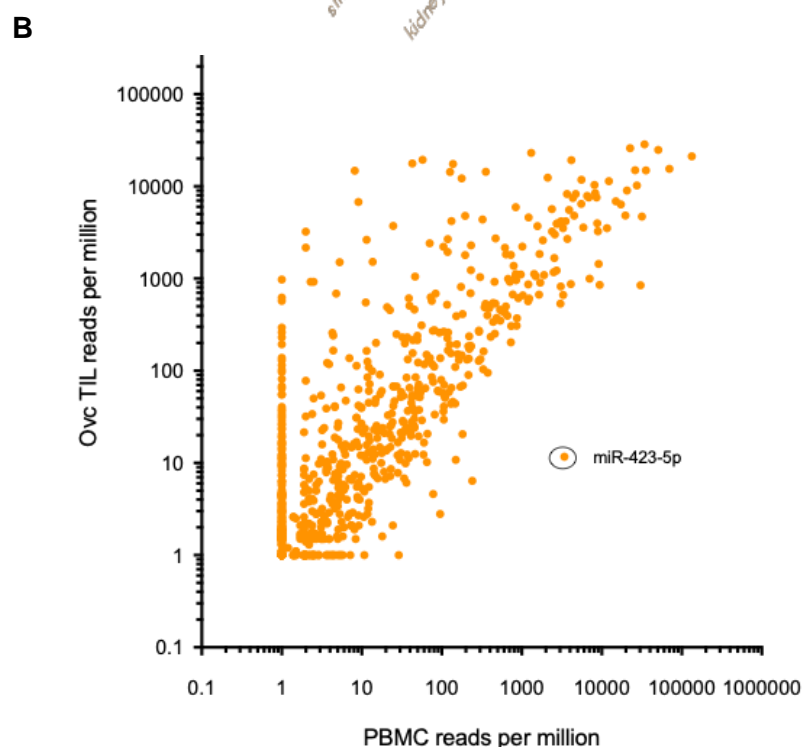
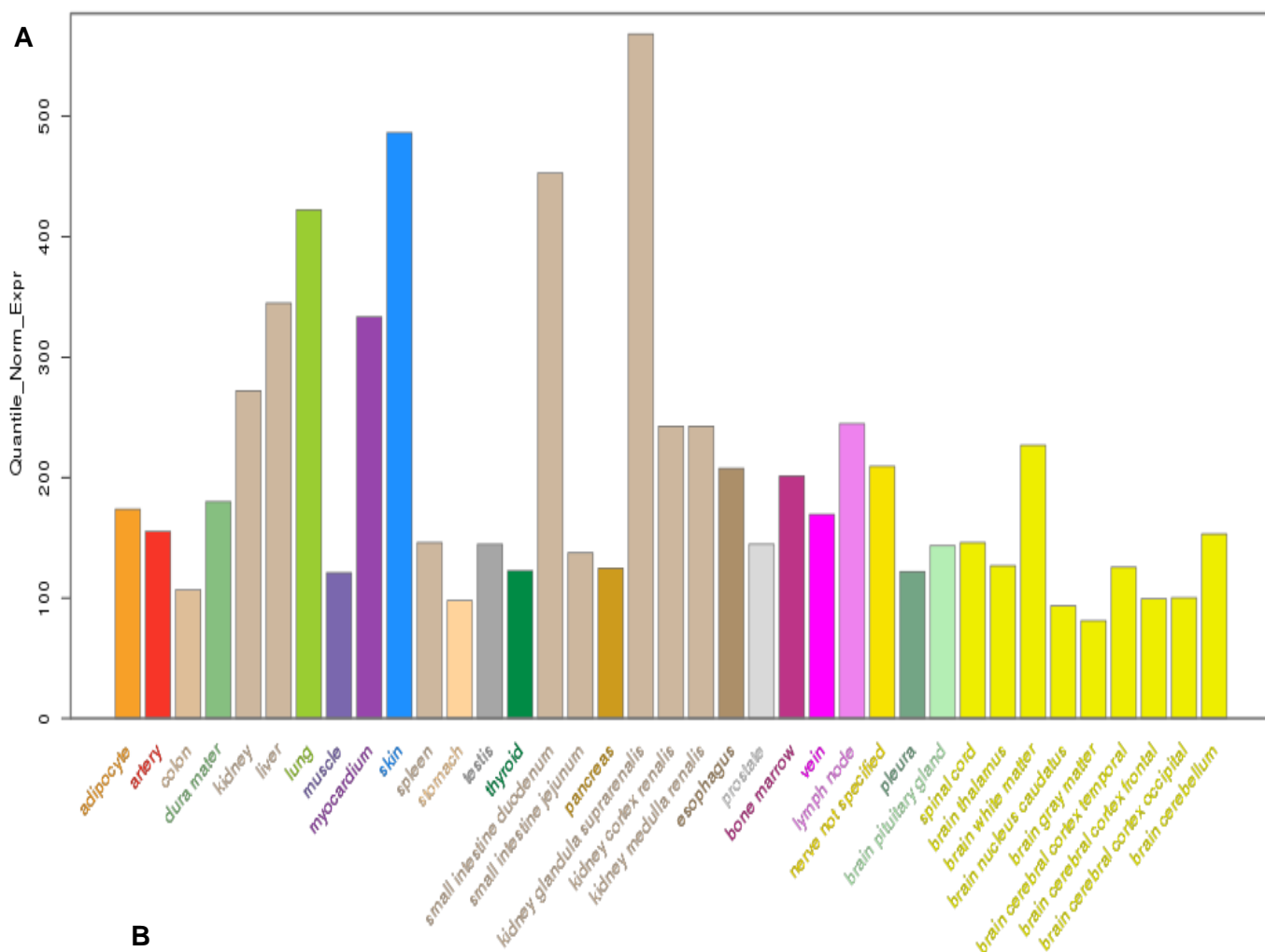


Supplementary Fig.S4. GFP expression in tumor-infiltrating leukocytes after in vivo HSPC transduction (TC-1 model). *Continued on next page.*

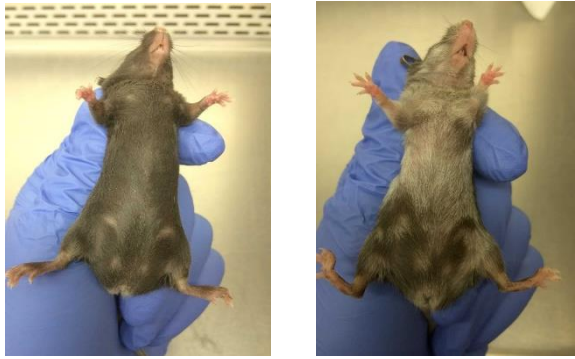
Supplementary Fig.S4. GFP expression in tumor-infiltrating leukocytes after in vivo HSPC transduction (TC-1 model). **A)** Schematic of the experiment. HSPCs were mobilized in CD46tg transgenic mice by s.c. injections of human recombinant G-CSF (5 µg/mouse/day, 4 days) followed by an s.c. injection of AMD3100 (5 mg/kg) eighteen hours after the last G-CSF injection. A total of 8×10^{10} viral particles of HDAd-GFP/mgmt+HDAd-SB were injected i.v. one hour after AMD3100. To prevent pro-inflammatory cytokine release after HDAd injection, animals received Dexamethasone (10 mg/kg) i.p. 16 h and 2 h before virus injection. Six weeks later, three rounds of O⁶BG/BCNU (i.p.) were applied to activate the exit of transduced HSPCs into the peripheral blood circulation (30 mg/kg O6BG plus 5, 7.5, and 10 mg/kg BCNU. 17 weeks after in vivo transduction, 5×10^4 TC-1 cells were implanted into the mammary fat pad. Five weeks later, tumors and other tissues were harvested and analyzed for GFP expression. **B)** Percentage of GFP-expressing PBMCs at different time points after in vivo transduction. Each symbol represents an individual animal. **C)** Percentage of GFP+ cells in cells stained for the pan-leukocyte marker CD45 in bone marrow, spleen, blood, and collagenase/dispase-digested tumor. **D)** Representative flow cytometry data of GFP+ cells in total (malignant + tumor infiltrating) cells and of GFP+ positive leukocytes. **E).** Representative tumor section. Left panel: GFP fluorescence. Right panel: staining with antibodies against GFP (green) and the extracellular matrix protein laminin (red). The scale bar is 50 µm. **F)** Immunophenotyping of GFP+ cells in the tumor and PBMCs in blood. Lymphocyte flow cytometry panel 8c (CD45, CD3, CD4, CD8, CD25, CD19) and myeloid panel 9c (CD45, CD11c, F4/80, MHCII, SiglecF-PecCP, Ly6C, CD11b, Ly6G) from BD Biosciences were used.



Supplementary Fig. S5. Validation of miR-423-5p expression by Northern blot. Total RNA (2 μ g) from bone marrow lineage-negative cells, spleen, total blood cells, and MMC-/TC-1-tumor infiltrating leukocytes was separated in 15% denaturing polyacrylamide gel and blots were hybridized with a probe specific for miRNA-423-5p and subsequently with a probe for U6 RNA (as loading control). Mir-423 has a precursor length of ~70bp and a mature miRNA length of 23bp. miR-423-5p-specific signals are visible for blood, bone marrow, and spleen, but absent in tumor-infiltrating cells in both tumor models.



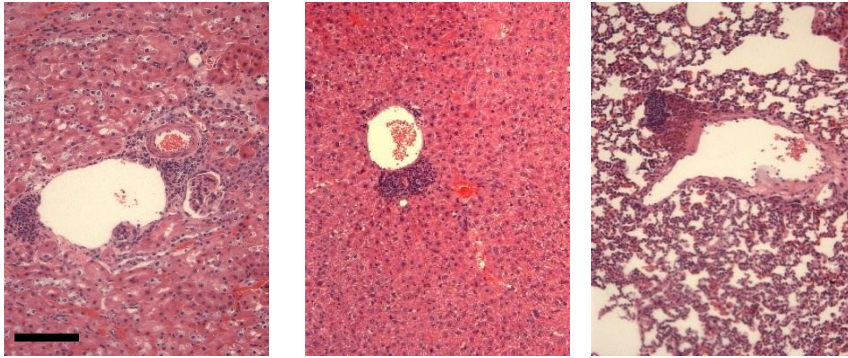
Supplementary Fig.S6. miRNA423-5p expression in humans. A) Levels of miR-423-5p in a published data set (see ref. 28). **B)** Plotted miRNA-Seq data from two ovarian cancer patients (pooled). CD45+ cells were isolated from biopsies of high-grade serous ovarian. RNA was isolated from tumor-infiltrating leukocytes and matching PBMCs and subjected to miRNA-Seq by LC Sciences, LLC. miRNA-423-5p is indicated

A**B**

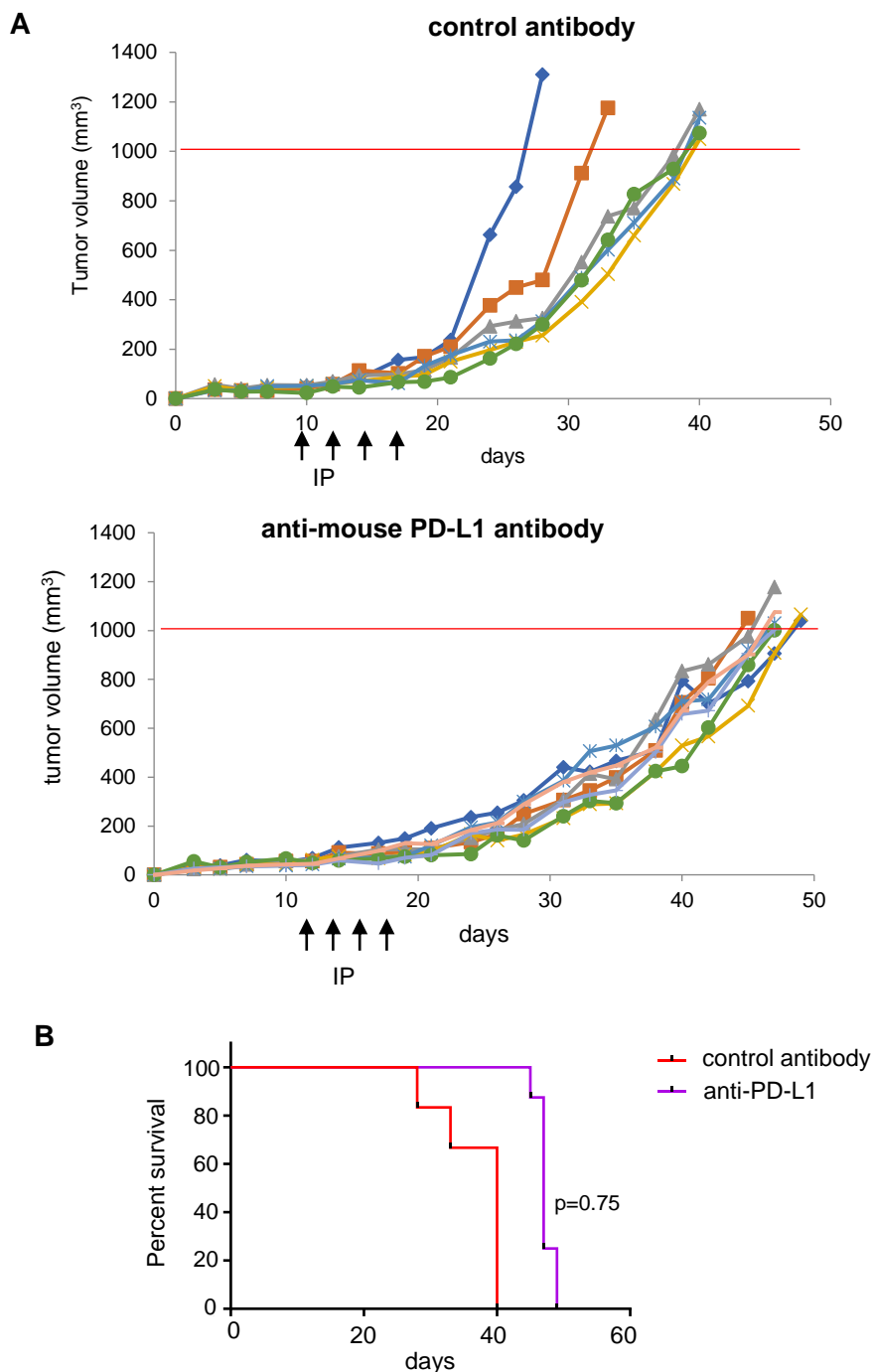
kidney

liver

lung

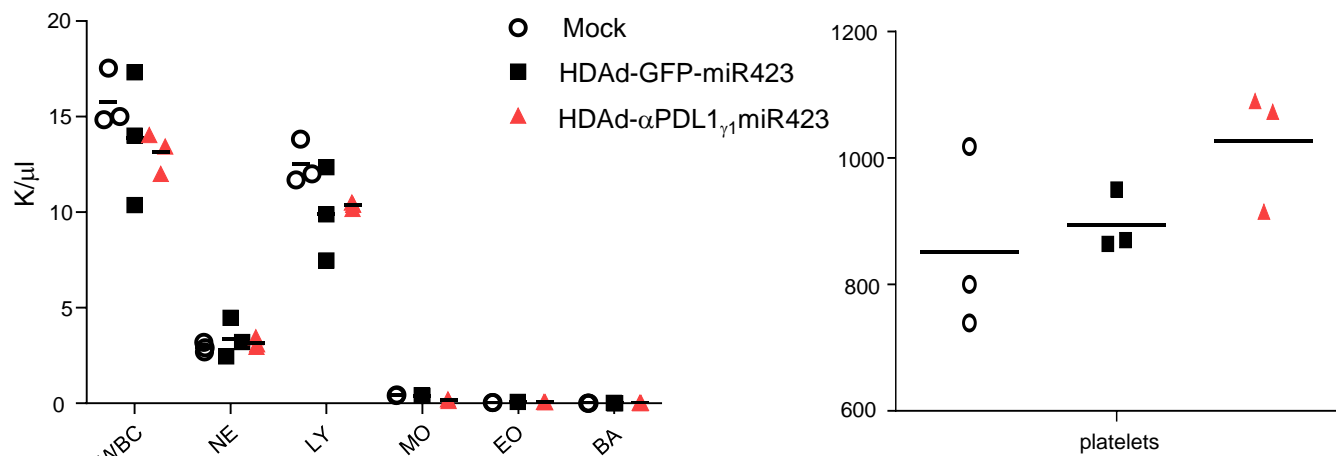
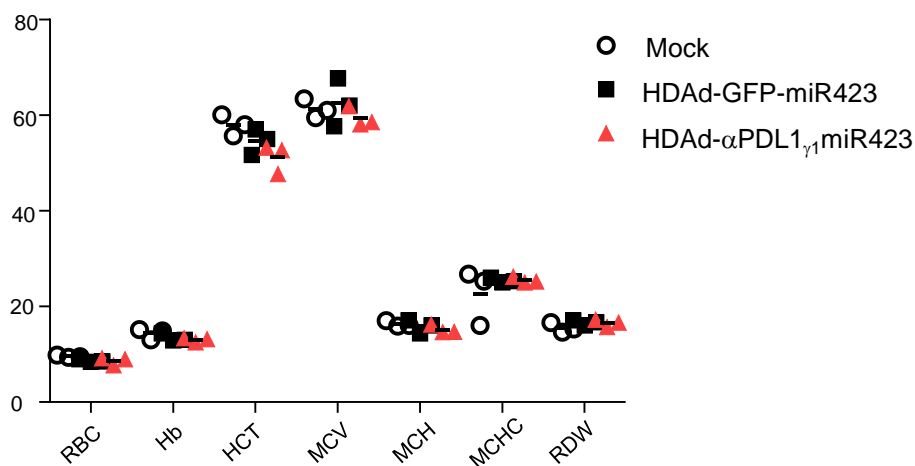


Supplementary Fig. S7. Autoimmune reactions in animals sacrificed at day 17 at the peak of α PDL1- γ_1 , before reversal of tumor growth. A) Fur discoloration in a treated animal (right panel) compared to an animal before treatment (left panel). **B)** Histological analysis of organs from a treated animal. Sections were stained with H&E. Shown are representative areas. The scale bar is 20 μ m. Note the infiltrates of mononuclear cells.



Supplementary Fig. S8. Effect of anti-PDL1 monoclonal antibody therapy in neu-transgenic mice with MMC tumors. When tumors reached a volume of 100mm³, mice received intraperitoneal injections of the anti-mouse PD1-L1 monoclonal antibody muDX400* (5 mg/kg i.p.) (4x every 4 days) or an isotype control antibody. **A)** Shown is the tumor volume in individual mice. **B)** Kaplan-Meier survival plot. Tumors with a volume of 1000mm³ were taken as endpoint. The difference between the two groups is not significant.

*Brunn ND, Mauze S, Gu D, et al. The Role of Anti-Drug Antibodies in the Pharmacokinetics, Disposition, Target Engagement, and Efficacy of a GITR Agonist Monoclonal Antibody in Mice. *J Pharmacol Exp Ther.* 2016;356: 574-586.

A**B**

Supplementary Fig. S9. Effect of in vivo HSC transduction on hemopoiesis. A) Blood cell counts in hCD46-transgenic mice shown in Fig.6D at week 2 after in vivo HSCPC transduction **B)** Hematological parameters. RBC: red blood cells, Hb: hemoglobin, MCV: mean corpuscular volume, MCH: mean corpuscular hemoglobin, MCHC: mean corpuscular hemoglobin concentration, RDW: red cell distribution width. Statistical analysis was performed using two-way ANOVA. The differences between the three groups were not significant.

Supplementary Methods

Construction of the HDAd-GFP/mgmt and HDAd- α PD-L1 γ_1 vectors: Step 1: The PGK promoter, β -globin 3' UTR and BGH polyA fragments were PCR amplified from pHCA-HBG-CRISPR/mgmt¹, followed by insertion into the BstBI site of pBS-Z-Ef1 α ² by Gibson assembly (New England Biolabs), generating pBS-PGK-3'UTR. The GFP coding sequence was PCR amplified from pHM5-frt-IR-Ef1 α -mgmt-2a-GFP³ and ligated with EcoRI linearized pBS-PGK-3'UTR, generating pBS-PGK-GFP. Step 2: The Ef1 α -mgmt^{P140K}-SV40pA-cHS4 insulator cassette was amplified from pHM5-T/ μ LCR- γ -globin-mgmt-FRT2⁴ and ligated with PacI-digested pHM5-T/ μ LCR- γ -globin-mgmt-FRT2, forming pHM5-FRT-IR-Ef1 α -mgmt. A BsrGI site at 3' side of cHS4 was introduced by primer for downstream use. The bacterium plasmid backbone of pHM5-FRT-IR-Ef1 α -mgmt was switched to the backbone from pBS-Z-Ef1 α using primers containing 15 bp homology arm (HA) for later infusion cloning (Takara, Mountain View, CA), generating pBS-FRT-IR-Ef1 α -mgmt. The two 15 bp HAs flanking the two Frt-IR components can be exposed upon PacI digestion to facilitate recombination with the modified pHCA construct described below. Then, the PGK-GFP-3'UTR-BGHpA fragment was moved from pBS-PGK-GFP in step 1 to the BsrGI site of pBS-FRT-IR-Ef1 α -mgmt, generating pBS-FRT-IR-GFP/mgmt. Step 3: The original PacI site in pHCA was destroyed by inserting two annealed oligo sequences. A new PacI site together with two HAs were created at BstBI site. Finally, after PacI digestion of both pBS-FRT-IR-GFP/mgmt and modified pHCA, the products were recombined by infusion cloning, generating pHCA-FRT-IR-GFP/mgmt, which was used for subsequent virus rescue. HDAd- α PD-L1 γ_1 was constructed similarly as HDAd-GFP/mgmt described above, except instead of GFP coding sequence, the anti-PD-L1- γ_1 transgene was inserted into the EcoRI of pBS-PGK-3'UTR at step 1. For microRNA regulated gene expression, synthesized 4 \times miR423 oligos (forward, 5'-CTAGGAAAGTCTCGCTCTCTGCCCTCATCACAAGTCTCGCTCTCTGCCCTCACGATAAAGTCTCGCTCTCTGCCCTCATTCAAAGTCTCGCTCTCTGCCCTCAC-3'; reverse, TCGAGTGAGGGGCGAGAGCGAGACTTTTGAATGAGGGGCGAGAGCGAGACTTTATCGTGAGGGGCGAGAGCGAGACTTTGTGATGAGGGGCGAGAGCGAGACTTTC) were annealed and inserted into the AvrII-XhoI sites of pBS-PGK-3'UTR, generating pBS-PGK-miR423-3'UTR, which was then used for anti-PD-L1- γ_1 insertion. HDAd-GFP-423 was constructed in a similar way by inserting the 4 \times miR423 target sites into the 3'UTR of HDAd-GFP/mgmt.

Flow cytometry: Cells were resuspended at 1×10^6 cells/100 μ L in PBS supplemented with 1 % FCS and incubated with FcR blocking reagent (Miltenyi Biotech, Auburn CA) for ten minutes on ice. Next the staining antibody solution was added at 100 μ L per 10^6 cells and incubated on ice for 30 minutes in the dark. After incubation, cells were washed once in FACS buffer (PBS, 1%FBS). For secondary staining the staining step was repeated with a secondary staining solution. After the wash, cells were resuspended in FACS buffer and analyzed using a LSRII flow cytometer (BD Biosciences, San Jose, CA). Debris was excluded using a forward scatter-area and sideward scatter-area gate. Single cells were then gated using a forward scatter-height and forward scatter-width gate. Flow cytometry data were then analyzed using FlowJo (version 10.0.8, FlowJo, LLC). Matched isotype-controls were included in all experiments.

Flow cytometry for immunophenotyping: Lymphocyte flow cytometry panel 8c (CD45-APC/Cy7, clone 30-F11, cat# 103116; CD3-APC, clone 17A2, cat# 100236; CD4-PE/Cy7, clone GK1.5, cat# 100422; CD8a-PE, clone 53-6.7, cat# 100708; CD25-BV421, clone PC61, cat# 102043; CD19-BV510, clone 6D5, cat# 115546; all these antibodies were from Biolegend) and myeloid panel 9c (CD45-APC/Cy7, clone 30-F11, Biolegend, cat# 103116; CD11c-APC, clone N418, Biolegend, cat# 117310; F4/80-PE, clone C1:A3-1, Cedarlane, cat# CL8940PE; MHCII-BV510, clone M5/114.15.2, Biolegend, cat# 107635; Siglec F-PerCP, clone 1RNM44N, eBioscience, cat# 46-1702-82; Ly6C-BV421, clone AL-21, BD Biosciences, cat# 562727; CD11b-PE/Cy7,

clone M1/70, eBioscience, cat# 25-0112-82; Ly6G-BV605, clone 1A8, Biolegend, cat# 127639) were used. The gating strategy is shown in Suppl. Fig. S2. LSK (lineage⁻/Sca-1⁺/c-Kit⁺) cells were characterized previously⁵. The following antibodies were also used: biotin-conjugated lineage detection cocktail (Miltenyi Biotec, San Diego, cat#130-092-613); anti-mouse LY-6A/E (Sca-1)-PE-Cyanine7 (clone D7, eBioscience, San Diego, cat# 25-5981-82); anti-mouse CD117 (c-Kit)-PE (Clone 2B8, eBioscience, San Diego, cat# 12-1171-83); anti-mouse CD3-APC (clone 17A2, Invitrogen, Waltham, MA, cat# 17-0032-82); anti-mouse CD19-PE-Cyanine7 (clone eBio1D3, eBioscience, San Diego, cat# 25-0193-82); anti-mouse Ly-6G (Gr-1)-PE, (clone RB6-8C5, eBioscience, San Diego, CA, cat #12-5931-82); anti-human CD46-APC (clone E4.3, BD Pharmingen, San Diego, CA, cat# 564253).

IFN γ -flow cytometry: Splenocytes were isolated by passing freshly harvested spleen through a 70 μ m cell strainer attached to a 50 mL Falcon tube. After centrifugation at 300 \times g for 10 minutes, red blood cells were removed by resuspending cells in 1 mL 1 \times BD Pharm Lyse™ lysing solution (BD Pharmingen, San Diego, CA, cat# 555899) and incubating for 30 seconds. 20 mL RPMI-1640 medium was added to stop lysing reaction. Following centrifugation and resuspension in RPMI-1640 medium with 10% heat-inactivated FBS, 100 units/ml penicillin and 100 mg/ml streptomycin, the obtained splenocytes were cultured at 5 \times 10⁶ cells/ml (200 μ l/well) in 96-well tissue culture plates in a humidified incubator with 5% CO₂. 1 \times Cell Stimulation Cocktail plus protein transport inhibitors (eBioscience, San Diego, cat# 00-4975-93) was presented in the culture medium for induction and accumulation of IFN- γ production within the cells. After stimulation for 12 hours, the cells were collected, stained first with cell surface markers as described above, and then subject to intracellular staining for IFN- γ (Biolegend, San Diego, CA, cat# 505842) according to the manufacturer's instructions.

Neu-tetramer flow cytometry: The PE-labeled H-2Dq/RNEU420–429 (H-2D(q) PDSLRDLSVF) tetramer was obtained from the National Institute of Allergy and Infectious Diseases MHC Tetramer Core Facility (Atlanta, GA), and used according to the manufacturer's instructions.

Isolation of tumor-infiltrating leukocytes for flow cytometry, FACS, and Western blot: Mice were sacrificed when tumor volume reached 500 mm³. Tumors were harvested, diced and digested with 300 U/mL Collagenase I (Sigma-Aldrich, St. Louis, MO, cat# C0130) and 1 mg/mL Dispase II (Sigma-Aldrich, cat# 4942078001) in 5 mL of RPMI 1640 for 30 minutes at 37°C with gentle mixing. After digestion, 2000 U/mL DNase I (Sigma-Aldrich, cat# 260913) was added to reduce viscosity by removing released DNA. Single cell suspension was obtained by passing the digested tissue through a 70 μ m cell strainer using a syringe plunger. Subsequently, tumor infiltrating leukocytes were purified from the single cell suspension using mouse CD45 (TIL) MicroBeads (Miltenyi Biotec, Auburn CA, cat# 130-110-618).

Immunofluorescence studies: Tumor slides were fixed with acetone/methanol (10 min) and washed twice with PBS. Slides were blocked for 20 min at room temperature using PBS with 5% blotting grade milk (Bio-Rad, Hercules, CA) followed by incubation with primary antibodies in PBS for 1 h at room temperature. Then slides were washed twice with PBS and incubated with secondary antibodies for 1 h at room temperature followed by washing with PBS three times. Slides were washed twice with PBS, mounted with Mounting Medium for Fluorescence (Vector Laboratories Burlingame, CA) and then analyzed using a fluorescence microscope. Laminin was detected using anti-laminin polyclonal (primary) antibody (1:200; #Z0097; Dako, Carpinteria, CA) and goat anti-rabbit IgG Alexa Fluor568 (secondary) antibody (1:200; Molecular Probes, Carlsbad, CA).

Immunohistochemistry of mouse tissues: Tissues were fixed in 10% formalin and processed for hematoxylin and eosin staining. All samples were examined by two experienced pathologists for typical inflammation signs in a blinded manner.

T-cell assays: MMC cells (Neu-positive) and splenocytes from syngeneic neu/CD46-transgenic mice (Neu-negative) were treated with mitomycin C at a final concentration of 50 µg/m for 20 min, and then washed extensively. Splenocytes from test animals (HDAd-αPD-L1-γ₁ treated) and untreated control animals (naïve) were mixed 1:1 with mitomycin C treated cells and incubated for 1 day in the presence of 10 U/ml IL-2. Control splenocytes were also treated with PMA/ionomycin. IFNγ concentrations in the supernatant were measured by IFNγ ELISA (Invitrogen, cat#88-7214-22)

MicroRNA array analysis was performed by the UW Functional Genomics, Proteomics & Metabolomics Facility Core using Affymetrix miRNA 4.0 arrays

Real-time PCR: Total RNA was extracted from tumor infiltrating leukocytes, PBMCs, splenocytes and bone marrow cells using TRIzol per manufacturer's instructions (Invitrogen), then reverse transcribed to generate cDNA using QuantiTect Reverse Transcription Kit from Qiagen (cat# 205311). The gDNA wipe-out reagent provided in the kit was used to eliminate potential genomic DNA contamination. Comparative real-time PCR was performed using Power SYBR Green PCR master mix (Applied Biosystems). The following primers were used: anti-mouse PDL1 forward, 5'-GGTTCAGCCTGGTGGGTCTTTG-3', and reverse, 5'-ATCTGGAGGTATGCGGTGTTCTTC-3'; mouse PPIA forward, 5'-GCATACAGGTCCTGGCATCT-3', and reverse, 5'-ATCCAGCCATTCACTCTTGG-3'; mouse RPL10 forward, 5'-TGAAGACATGGTTGCTGAGAAG-3', and reverse, 5'-GAACGATTTGGTAGGGTATAGGAG-3'. Mouse *PPIA* was used as an internal control. A second internal control mouse *RPL10* was also included and similar results were observed. Results were calculated according to $2^{(-\Delta\Delta Ct)}$ method and presented as percentage of relative expression, with setting the cDNA level of corresponding tumor samples as 100%.

Isolation of lineage-depleted (Lin⁻) bone marrow cells: For the depletion of lineage-committed cells, the mouse lineage cell depletion kit (Miltenyi Biotec, San Diego, CA) was used according to the manufacturer's instructions.

Colony forming unit assay. A total of 2500 Lin⁻ cells were plated in triplicates in ColonyGEL 1202 mouse complete medium (ReachBio, Seattle WA) and incubated for 12 days at 37 °C in 5 % CO₂ and maximum humidity. Colonies were enumerated using a Leica MS 5 dissection microscope (Leica Microsystems).

References:

1. Li C, Psatha N, Sova P, et al. Reactivation of gamma-globin in adult beta-YAC mice after ex vivo and in vivo hematopoietic stem cell genome editing. *Blood*. 2018;131: 2915-2928.
2. Saydaminova K, Ye X, Wang H, et al. Efficient genome editing in hematopoietic stem cells with helper-dependent Ad5/35 vectors expressing site-specific endonucleases under microRNA regulation. *Mol Ther Methods Clin Dev*. 2015;1: 14057.
3. Wang H, Richter M, Psatha N, et al. A Combined In Vivo HSC Transduction/Selection Approach Results in Efficient and Stable Gene Expression in Peripheral Blood Cells in Mice. *Mol Ther Methods Clin Dev*. 2018;8: 52-64.
4. Li C, Psatha N, Wang H, et al. Integrating HDAd5/35++ Vectors as a New Platform for HSC Gene Therapy of Hemoglobinopathies. *Mol Ther Methods Clin Dev*. 2018;9: 142-152.
5. Richter M, Saydaminova K, Yumul R, et al. In vivo transduction of primitive mobilized hematopoietic stem cells after intravenous injection of integrating adenovirus vectors. *Blood*. 2016;128: 2206-2217.